J Nanopart Res (2015) 17:410
DOI 10.1007/s11051-015-3210-3

RESEARCH PAPER

Silica nanoparticles and biological dispersants: genotoxic effects on A549 lung epithelial cells

David M. Brown · Julia Varet · Helinor Johnston · Alison Chrystie · Vicki Stone

Received: 9 October 2014 / Accepted: 5 October 2015 / Published online: 16 October 2015

Abstract Silica nanoparticle exposure could be intentional (e.g. medical application or food) or accidental (e.g. occupational inhalation). On entering the body, particles become coated with specific proteins depending on the route of entry. The ability of silica particles of different size and charge (non-functionalized 50 and 200 nm and aminated 50 and 200 nm) to cause genotoxic effects in A549 lung epithelial cells was investigated. Using the modified comet assay and the micronucleus assay, we examined the effect of suspending the particles in different dispersion media [RPMI or Hanks' balanced salt solution (HBSS), supplemented with bovine serum albumin (BSA), lung lining fluid (LLF) or serum] to determine if this influenced the particle's activity. Particle characterisation suggested that the particles were reasonably well dispersed in the different media, with the exception of aminated 50 nm particles which showed evidence of agglomeration. Plain 50, 200 nm and aminated 50 nm particles caused significant genotoxic effects in the presence of formamidopyrimidine-DNA glycosylase when dispersed in HBSS or LLF. These effects were reduced when the particles were dispersed in BSA and serum. There was no significant micronucleus formation produced by any of the particles when suspended in any of the dispersants. The data suggest that silica particles can produce a significant genotoxic effect according to the comet assay in A549 cells, possibly driven by an oxidative stress-dependent mechanism which may be modified depending on the choice of dispersant employed.

Keywords Genotoxicity · Nanoparticles · A549 · Lung lining fluid · Dispersant · Colloids · Environmental and health issues

Electronic supplementary material The online version of this article (doi:10.1007/s11051-015-3210-3) contains supplementary material, which is available to authorized users.

D. M. Brown (✉) · H. Johnston · A. Chrystie · V. Stone
Nanosafety Research Group, School of Life Sciences, Heriot-Watt University, Riccarton, Edinburgh EH14 4AS, UK
e-mail: d.brown@hw.ac.uk

H. Johnston
e-mail: h.johnston@hw.ac.uk

V. Stone
e-mail: v.stone@hw.ac.uk

J. Varet
Institute of Occupational Medicine, Riccarton, Edinburgh EH14 4AP, UK
e-mail: julia.varet@IOM-world.org

Introduction

With the increased use of nanoparticles (NPs), the likelihood of human exposure is expected to rise in consumer, occupational and environmental settings, and an understanding of the potential risk to human health is essential (Balbus et al. 2007). Currently, information regarding the exposure risks to workers or

consumers is limited. NPs may enter the body via a number of routes, for example, inhalation, ingestion, dermal absorption or by injection in a clinical setting. There is evidence that NPs may cross the epithelial barrier of the lung (Oberdorster et al. 2002), gastrointestinal tract (Jani et al. 1990; Schleh et al. 2012) and ultimately sequester in sites throughout the body (Lipka et al. 2010). Therefore, the toxic effects of NPs may be widely distributed (Oberdorster et al. 2005). Nanoparticles inhaled into the lungs encounter lung lining fluid (LLF) which is a complex mixture of phospholipids and proteins and has been shown to possess important immunoregulatory effects on cells (Wilsher et al. 1988). In contrast, nanoparticles entering the circulatory system, either by translocation or by injection, interact with serum proteins (Casals and Puntes 2012; Ehrenberg et al. 2009). In vitro models of lung cells frequently contain serum and therefore do not represent the composition of LLF. It is therefore relevant to ascertain the influence of serum on lung cells and responses to NPs in order to determine the model's limitations.

Previous studies have demonstrated that NPs are readily coated in vitro with proteins of various compositions (Brown et al. 2012; Lundqvist et al. 2011) and that protein enhances the inflammogenicity of multi-walled carbon nanotubes (MWCNTs) in vivo (Rothen-Rutishauser et al. 2010). Bound proteins and other materials may alter the particle reactivity and hence may mask their true toxicity. It is unclear whether 'bound' bioactive molecules retain their functionality, or conversely become less functional or inert due to conformational changes once they become 'bound'. In previous studies, we have demonstrated that pro-inflammatory cytokines such as IL-8 and TNF-α lose some of their biological activities when adsorbed to 14 nm carbon black (CB), and also that the CB loses some of its biological effects as a consequence of this interaction (Brown et al. 2012). As part of the present study, we report the differential effects of silica particles dispersed in cell culture medium or HBSS supplemented with albumin, serum and LLF with respect to their genotoxic impacts on A549 lung epithelial cells. We chose silica particles with different surface chemistries and particle size (non-functionalized (uncharged) and aminated, 50 and 200 nm diameter) to allow the identification of the physical and chemical properties of NPs that influence their interaction with proteins. Silica particles have been used in medical imaging techniques because they can be easily bio-functionalized. They also possess stable and porous properties which makes them ideal materials for carriers of high-contrast imaging dyes. We chose aminated particles which would be expected to impart a positive charge. Charge has been reported to play a role in binding biological molecules and consequently how efficiently the particles are phagocytosed and cleared (Nel et al. 2009) and is also often associated with greater toxicity (Fröhlich 2012).

We have previously shown that some NPs exert their toxicity towards cells at least in part, through an oxidative stress mechanism (Brown et al. 2001; Stone et al. 1998). The use of the modified comet assay to investigate the role of reactive oxygen species (ROS) using silica NPs dispersed in different biological media was used here to give a clearer understanding of the particle toxicity. The enzyme formamidopyrimidine-DNA glycosylase (Fpg) is important in the base excision pathway and is involved in the excision of modified purine bases, in particular those which are the result of oxidative damage (Seeberg et al. 1995). Hence, oxidative damage to DNA can be detected and, for this reason, this enzyme was included in the modified comet assay.

In this study, our aim was to investigate the influence of different dispersants on the genotoxicity of silica NPs, in A549 lung epithelial cells. Particles entering the lung can cause inflammation and as a result components present in the blood such as serum and albumin may enter the airspaces from the pulmonary circulation. The particles themselves initially become coated with components of lung lining fluid and then coated with serum components or albumin. We chose albumin and serum as dispersants because of their relevance to in vitro culture conditions with respect to exposure of organ systems to blood-borne NPs, and lung lining fluid due to its mixed phospholipid and protein composition and its relevance to exposure to NPs via the lung.

Materials and methods

Particle characterisation

The material used in this study consisted of silica nanoparticles (50 and 200 nm diameter), one type with a neutral surface charge and a second type with an

expected positive (NH_2 modification) charge, obtained from Kisker Biotech, Steinfurt, Germany. NPs at twice the required concentration (highest concentration 62.5 μg/ml, equivalent to 16 μg/cm^2) were suspended in RPMI medium containing penicillin, streptomycin and L-glutamine (Sigma) and sonicated for 10 min. Dispersants consisted of solutions of medium alone, 0.1 % bovine serum albumin (BSA) (Sigma), 1 μg protein/ml lung lining fluid (LLF) (see below for preparation) and 0.1 % heat-inactivated foetal calf serum, and each dispersant was diluted to twice the required concentration in RPMI medium. Particle suspension and dispersant in equal amounts were mixed together and vortexed briefly prior to analysis by Dynamic Light Scattering (DLS). We also dispersed the particles in ultrapure water to the same final concentration used with the other dispersants. The hydrodynamic diameter and zeta potential of the NPs were determined using a Malvern nano ZS zetasizer, according to the manufacturer's protocol. According to the manufacturer's data, both of the aminated type particles had a surface charge of 1 μmol/g. This method of surface charge determination was based on polyelectrolyte titration, a modified acid base titration which allows the number of nmol of alkaline surface groups to be calculated and was carried out by the particle manufacturer.

Lung lining fluid (LLF) preparation

LLF was obtained from rat lungs according to the method of Baughman et al. (1987). The lungs from five male Sprague–Dawley rats, approximately 3 months old, were cannulated and removed, and lavaged with 4 × 8 ml volumes of sterile saline. Tubes were centrifuged at 258*g* for 5 min at 4 °C, and the supernatant collected. The supernatant was pooled, transferred into 50-ml centrifuge tubes and centrifuged at 250*g* for 10 min to remove remaining debris. The supernatant was then transferred to a 50 ml ultracentrifuge tube and centrifuged at 60,000*g* for 45 min. The resulting pellet was resuspended in 10 ml sterile PBS. This surfactant-enriched fraction, termed LLF, was aliquoted into 1 ml volumes and stored at −80 °C until required. The protein content of the LLF was determined using Biorad reagent (Biorad, Hertfordshire UK), according to the manufacturer's instructions, and used at a concentration of 1 μg/ml in medium or HBSS to disperse the NPs.

Preparation of particles for TEM

Silica particles and NPs were suspended in each of the dispersants at a concentration of 31.25 μg/ml as described above. 5 μl of each suspension was pipetted onto the surface of 200 mesh Formvar-coated copper grids (Agar Scientific) and allowed to dry at 37 °C for 24 h. The grids were coated with 5 nm of evaporated carbon prior to imaging. An FEI Tecnai TF20 FEGTEM microscope fitted with a Gatan Orius SC600 CCD camera was used to image the particles.

A549 cell culture and treatments

Comet assay treatments

A549 epithelial cells were grown in continuous culture in RPMI-1640 medium (Sigma) containing L-glutamine (diluted from 100 × stock solution, Life Technologies, to give a final concentration of 2 mM), penicillin (100 U, Sigma) and streptomycin (100 μg/ml, Sigma) and 10 % heat-inactivated foetal calf serum (complete medium). The cells were washed with 25 ml sterile saline after which 5 ml trypsin (Sigma, diluted from 100 × stock in sterile saline) was added to the flasks and incubated for 5 min at 37 °C, 5 % CO_2. Ten millilitres of complete medium was added to each flask and the cells released by gentle shaking. Cells were counted and plated into 6-well plates at 2 × 10^5 cells/ml (3 ml/well). Plates were incubated for 24 h at 37 °C, 5 % CO_2, wells were washed with a 3 ml volume of HBSS, and treatments were added to each well in a final volume of 3 ml in HBSS (Sigma). Treatments consisted of each particle type, or H_2O_2 (60 μM as a positive control) suspended (final concentration) in solutions of 0.1 % bovine serum albumin (BSA) (Sigma), 1 μg protein/ml lung lining fluid (LLF) and 0.1 % serum, all diluted in HBSS (Sigma) to a final concentration of 62.5 μg/ml. Non-functionalized particles were suspended in HBSS. In order to check that we were able to detect oxidative damage to DNA, an additional control consisting of the compound Ro-19-8022 (Roche), a substance which when activated by light produces oxidative damage to cells, was included. The compound was prepared in HBSS at a concentration of 0.4 μM and 3 ml added per well. The treatment well was exposed to a 1000 W halogen lamp for 2 min, after which the cells were harvested. All other

treatments were incubated for 4 h at 37 °C before being harvested for further investigation using the comet assay.

LDH assay treatments

A549 epithelial cells were cultured as described above and plated into 96-well plates at 2×10^5 cells/ml (200 µl/well) in complete medium and incubated for 24 h at 37 °C. Cells were then washed using 200 µl PBS and treated as described above, with the different particle types at concentrations ranging from 3.9 to 62.5 µg/ml suspended in the dispersants (made up in RPMI medium). 100 µl of each particle suspension and concentration was pipetted into triplicate groups of wells on a 96-well plate, and the plates were centrifuged at 716*g* for 2 min and then incubated at 37 °C for 4 and 24 h. Supernatants were removed and transferred to new sterile 96-well plates and stored at −80 °C until required. 100 µl of 0.1 % triton was added to each well of the plates containing the residual cells, and these were stored at −80 °C until required. This treatment was used to obtain a measure of 100 % lysis in the LDH assay.

LDH estimations

Fifty microlitres of 0.75 mM aqueous sodium pyruvate (Sigma) solution containing NADH (Sigma) at a concentration of 1 mg/ml was pipetted into each well of a 96-well plate and incubated at 37 °C for 5 min. A series of standards were prepared to give a range of dilutions representing 0–2000 Units/LDH/ml. 50 µl of pyruvate/NADH solution gave a concentration of 2000 LDH Units/ml. 10 µl of previously prepared cell supernatants (above) were added to the wells in triplicate groups and thoroughly mixed. In separate plates, 10 µl of the supernatant from the triton-treated cells was added. The plates were incubated for exactly 30 min at 37 °C. 50 µl of 2,4-dinitrophenylhydrazine (Sigma) solution dissolved in 1 M HCl (10 mg/dl) was added to each well and incubated at room temperature for 20 min. To develop the final colour, 50 µl of 4 M NaOH was added to each well, mixed and allowed to stand for 5 min. The absorbance was read at 540 nm on a Dynatech plate reader, and the number of units of LDH was calculated from a set of LDH standards included in the plate. The LDH content of the supernatants was expressed as a percentage of the 100 % lysis.

Comet assay

Cells were set up and treated as described above. After 4-h incubation, the treatments were removed and the cells were washed with HBSS solution. Cells were removed by trypsinization (as before), washed in 4 ml complete medium and resuspended in 1 ml complete medium. See supplemental data for the complete procedure. The Fpg enzyme activity was determined using the supplier's recommendations; the optimum concentration was 1 unit in 50 µl of Fpg buffer.

Micronucleus assay

A549 cells were set up in 24-well plates at a concentration of 1×10^5 cells/ml in RPMI medium containing 10 % FCS. Each well contained a 10 mm-diameter glass coverslip which had previously been sterilized using ethanol. 600 µl of cell suspension was dispensed into each well, and the plate was incubated for 24 h at 37 °C. On day 2, wells were washed with PBS and treatments in a volume of 500 µl added to wells in duplicate. Treatments consisted of the four silica particle types suspended in the different dispersants as described above (62.5 µg/ml final concentration), but this time made up in RPMI medium alone. One set of treatments consisted of mitomycin C (31.25 µg/ml) as a positive control for micronucleus formation. The treatments were incubated for 24 h at 37 °C. On day three, the treatments were removed, and the wells were washed with PBS and 500 µl RPMI medium containing 10 % FCS with cytochalasin B at a concentration of 4.5 µg/ml added to each well. The plate was incubated at 37 °C for a further 24 h, after which the wells were washed with PBS and the coverslips stained using Diffquick. The coverslips were allowed to dry and were mounted on glass microscope slides using DPX mounting medium.

Scoring

Slides were coded and scored blind to avoid scoring bias. Cells were counted by light microscopy using a 100× oil immersion objective lens. The micronuclei were scored using the criteria that MN are round or

oval structures similar to but smaller than the main nuclei. The MN should have no contact with main nucleus, have a size between 1/16 and 1/3 of the mean diameter of the main nucleus and have similar staining characteristics to the main nucleus. A minimum of 250 binucleated cells were counted per slide. In addition, mononucleated cells were counted, in order to calculate the cytokinesis block proliferation index (CBPI) to assess cell proliferation, using the following formula:

$$\begin{aligned}\text{CBPI} = {} & (\text{number of mononucleated cells} \\ & + 2 \times \text{number of binucleated cells} \\ & + 3 \times \text{number of trinucleated cells})/ \\ & \text{Total number of cells} \\ & (\text{as outlined by the OECD test 487}).\end{aligned}$$

Statistical analysis

Data from all experiments were analysed using the Minitab statistical package using a general linear model with subsequent analysis of variance and Tukey's test. Significance was set at 5 %.

Results

Particle characterisation

The DLS, polydispersity index (PDI), and zeta potential measurements of the particles dispersed in different media (and water) are shown in Tables 1, 2, 3 and 4.

The DLS measurements representing the hydrodynamic diameter of the silica NPs dispersed in various media are shown in Table 1. The size of the plain silica particles obtained by DLS suggested that very little particle agglomeration occurred when they were dispersed in medium, LLF and serum. The hydrodynamic diameter of all silica particles dispersed in BSA was in general smaller than reported by the manufacturer. However, the results reported in Table 1 are the mean diameter (nm) values and possibly do not correctly reflect the true size distribution of particles. Particle distribution graphs and data from all the particle types suspended in all of the dispersion media are included in supplementary material. These data suggest that the smaller particle sizes may be a result of the inclusion of measurements of aggregates of dispersant material. Aminated silica (50 nm) suspended in all dispersants apart from BSA produced measurements which were much larger than the reported size of the particles, suggesting that these particles were highly agglomerated, and the aminated 200 nm silica particles appeared to remain well dispersed in each medium type. The PDI data (Table 2) suggest that for BSA the range of agglomerate size is relatively broad reducing confidence in the hydrodynamic data (Table 1). The PDI values for the 50 nm aminated silica particles also suggest a broad size range in all media, especially albumin and serum.

Zeta potential measurements were low (Table 3), suggesting the potential of particles to agglomerate. Further analysis of the data indicated that there were no differences in the zeta potential of the particles themselves; however, there were significant differences among the dispersant types. The zeta potentials of particles dispersed in BSA and serum were significantly smaller than those of the particles dispersed in medium and LLF. Albumin and serum decreased the particle charge possibly due to the protein charge.

Table 1 DLS NP hydrodynamic diameters (mean ± SEM nm) of silica particles dispersed in a range of biological media (Bovine Serum Albumin (BSA 0.1 %), lung lining fluid (LLF 1 μg/ml) and serum 0.1 %)

Particle (nm)	Medium	BSA	LLF	Serum
Plain silica **50**	80.77 ± 1.14	34.68 ± 2.88	75.44 ± 1.02	80.13 ± 3.82
Plain silica **200**	192.43 ± 2.54	125.73 ± 0.19	208.9 ± 1.68	198 ± 2.21
Silica NH_2 **50**	348.07 ± 6.82	33.55 ± 1.03	297.7 ± 5.85	210.13 ± 8.11
Silica NH_2 **200**	205.97 ± 2.44	148.76 ± 0.29	217.27 ± 1.34	205.9 ± 2.57

The size values quoted in bold in column 1 of the table represent the values provided by the particle suppliers

Table 2 The polydispersity index (PDI) of silica NPs dispersed in a range of biological media

Particle (nm)	Medium	BSA	LLF	Serum
Plain silica **50**	0.396 ± 0.023	0.890 ± 0.033	0.276 ± 0.014	0.581 ± 0.064
Plain silica **200**	0.152 ± 0.007	0.617 ± 0.002	0.164 ± 0.006	0.248 ± 0.008
Silica NH_2 **50**	0.474 ± 0.037	0.999 ± 0.001	0.346 ± 0.038	0.848 ± 0.111
Silica NH_2 **200**	0.103 ± 0.029	0.585 ± 0.003	0.131 ± 0.011	0.189 ± 0.026

The size values quoted in bold in column 1 of the table represent the values provided by the particle suppliers

The criteria used to interpret these data are as follows: a value approaching 1 suggests a broad size distribution, indicative of large, sedimenting particles. The values > 0.5 suggest the presence of large and agglomerated particles

Table 3 The zeta potential of silica NPs dispersed in a range of biological media

Particle (nm)	Medium	BSA	LLF	Serum
Plain silica **50**	−20.57 ± 1.33	−17.63 ± 0.58	−23.07 ± 0.63	−12.57 ± 0.97
Plain silica **200**	−23.9 ± 1.16	−16.68 ± 0.44	−28.03 ± 0.35	−11.87 ± 0.07
Silica NH_2 **50**	−22.9 ± 0.93	−19.33 ± 1.00	−24.17 ± 0.56	−15.37 ± 0.32
Silica NH_2 **200**	−24.67 ± 1.23	−16.67 ± 0.38	−26.43 ± 1.56	−12.57 ± 0.64

The size values quoted in bold in column 1 of the table represent the values provided by the particle suppliers

The criteria used to interpret these data are as follows: 0 to ±5 indicates rapid coagulation/flocculation; ±10 to ±30 indicates incipient instability (Greenwood and Kendall 1999)

Table 4 DLS NP hydrodynamic diameters (mean ± SEM nm) of silica particles dispersed in water

Particle (nm)	Hydrodynamic diameter (nm)	Zeta potential (mV)
Plain silica **50**	52.11 ± 0.39	−19.6 ± 0.55
Plain silica **200**	208.4 ± 0.44	−34.37 ± 0.69
Silica NH_2 **50**	62.76 ± 0.35	−47.53 ± 1.06
Silica NH_2 **200**	205.83 ± 1.09	−28.97 ± 0.6

The size values quoted in bold in column 1 of the table represent the values provided by the particle suppliers

The particles measured in water (Table 4) were in the same size range as the values quoted by the manufacturer.

Figure 1a, b shows the images obtained by TEM of plain (P) 50 nm silica nanoparticles and NH_2-modified 50 nm nanoparticles dispersed in HBSS, BSA, LLF or serum. Images for the other particle sizes are not included here. The images show that the particles are not monodispersed regardless of the dispersant medium or surface charge.

Particle toxicity

Figure 2 shows the LDH release from A549 cells treated with silica NPs dispersed in medium, BSA, LLF or serum for 4 h.

After 4-h treatment with silica particles in different dispersants, according to the statistical analysis, there was no significant increase in LDH release at any dose compared with untreated cells suggesting that all doses were suitable for assessing genotoxicity. However, there appeared to be an increased LDH release at the highest dose of 62.5 μg/ml for particles dispersed in medium, LLF and serum, but these increases were not statistically significant. There was a large degree of variation associated with the data at this dose and time point, which may account for the lack of significance observed. In order to confirm a lack of toxicity, LDH release was also checked at 24 h (Fig. 3). Again no significant cytotoxicity was observed at 24 h.

Comet assay

Figure 4a, b summarises the % tail moment, a parameter illustrating the DNA strand breaks in

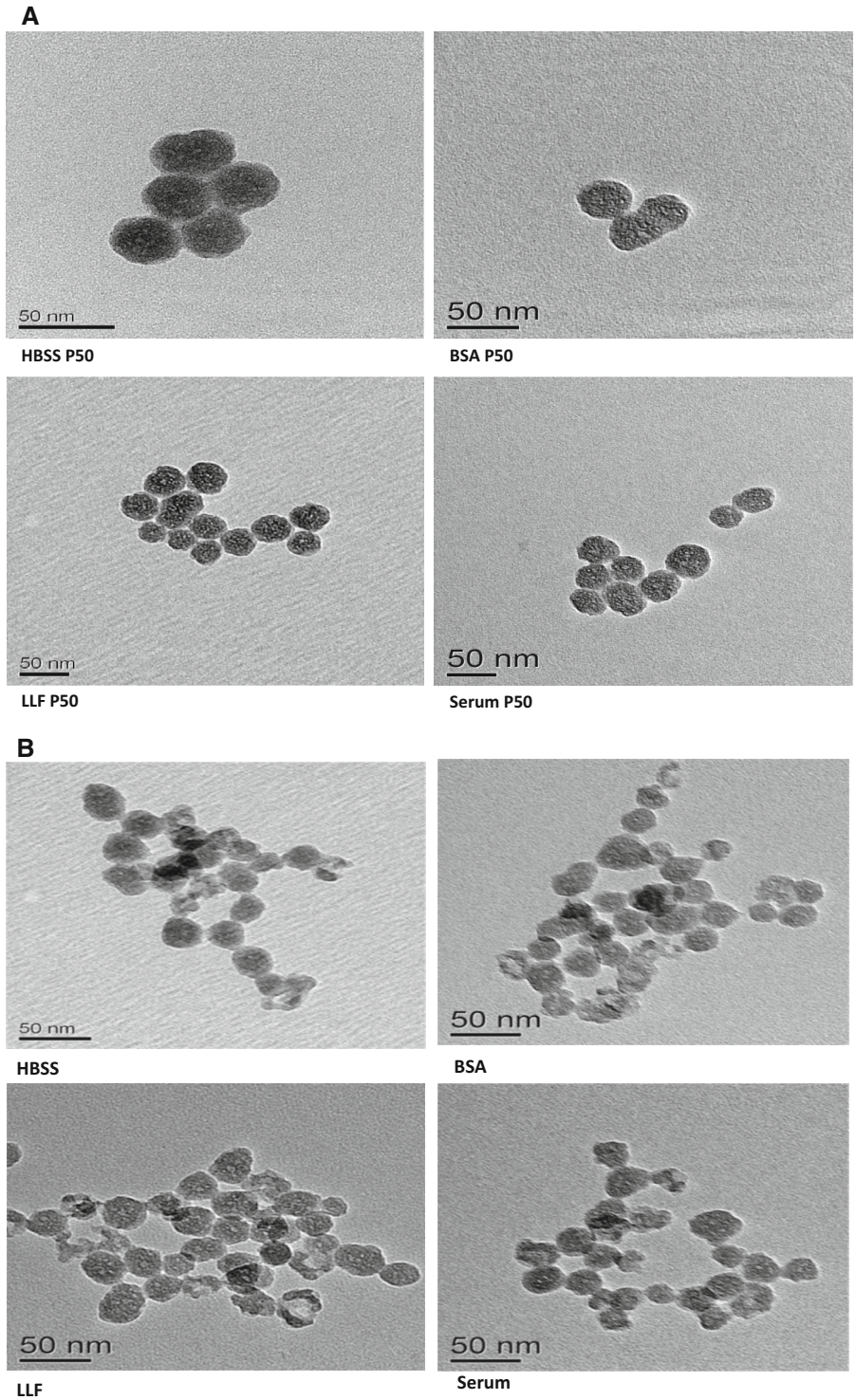

Fig. 1 TEM images of **a** plain 50 nm particles and **b** NH_2 50 nm surface-modified particles dispersed in different biological media

A549 epithelial cells, after treatment with silica NPs dispersed in different biological media. The addition of Fpg allows the identification of DNA damage associated with oxidation. Compound RO-198022 is a photosensitizer which induces specific oxidative damage in DNA after exposure to light. This compound

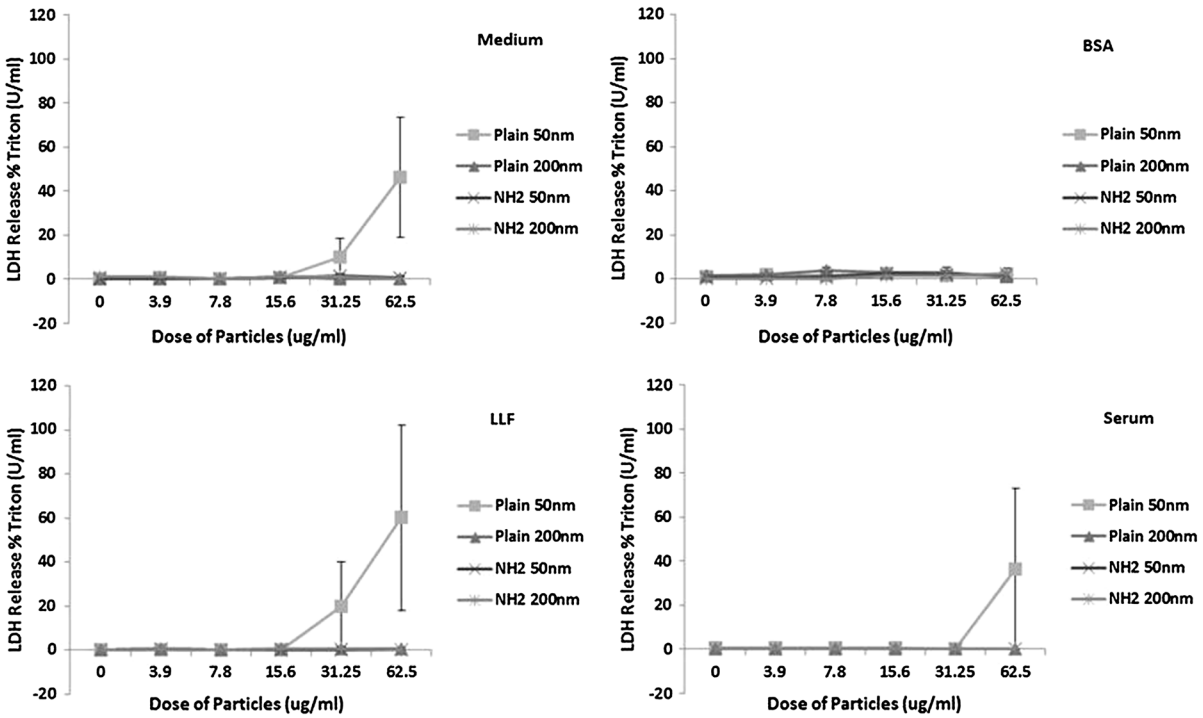

Fig. 2 LDH release from A549 cells treated with silica NPs dispersed in medium, BSA, LLF or serum for 4 h. Data represent the mean ± SEM of the number of units/ml of LDH released into the culture medium and expressed as a percentage of the total LDH remaining. Each experiment was carried out on three separate occasions

and H_2O_2 were included alongside the particle treatments as positive controls.

Figure 4a (upper graph) shows the controls included in the silica exposure experiments. Typically, incubating A549 cells in HBSS alone produced a tail moment of between 10 and 12 % in both Fpg- and non-Fpg-treated cells. Treatment for 4 h with 60 μM H_2O_2 increased the tail moment to between 16 % (no Fpg) and 18 % (plus Fpg). Treatment with RO-198022 compound increased the tail moment to approximately 25 % (no Fpg) and to 35 % for the Fpg treatment. Using ANOVA, there were significant differences between HBSS (control) and both H_2O_2 and RO-198022 compound and between H_2O_2 and RO-198022 compound ($p < 0.001$). There was a significant difference between treatment without the enzyme Fpg and treatment with Fpg only for the RO-198022 treatment ($p < 0.01$).

The lower graph in Fig. 4b shows the effect of silica particles in different dispersants. Examining each dispersant in turn, in HBSS, plain 50 nm silica NPs caused the largest increase in the tail moment compared with no particle treatment ($p < 0.001$ no Fpg treatment; $p < 0.05$ plus Fpg treatment). There was also a significant increase produced by aminated 50 nm NPs compared to the control ($p < 0.01$ no Fpg treatment; $p < 0.001$ plus Fpg treatment). Plain 200 nm particles in the presence of Fpg produced a significant increase in the tail moment ($p < 0.001$), this effect was not apparent in the absence of Fpg. The NH_2 200 nm particles had no effect.

There was no significant increase in the tail moment for any of the particle types compared with untreated cells when the particles were dispersed in BSA, either in the presence or in the absence of Fpg. However, some differences between the particle types themselves were observed (see Table 5).

When dispersed in LLF, only plain 50 nm and NH_2 50 nm silica nanoparticles produced a significant ($p < 0.001$) increase in the tail moment compared with untreated cells in the absence of Fpg. In the presence of Fpg, plain 50 nm, plain 200 nm and NH_2

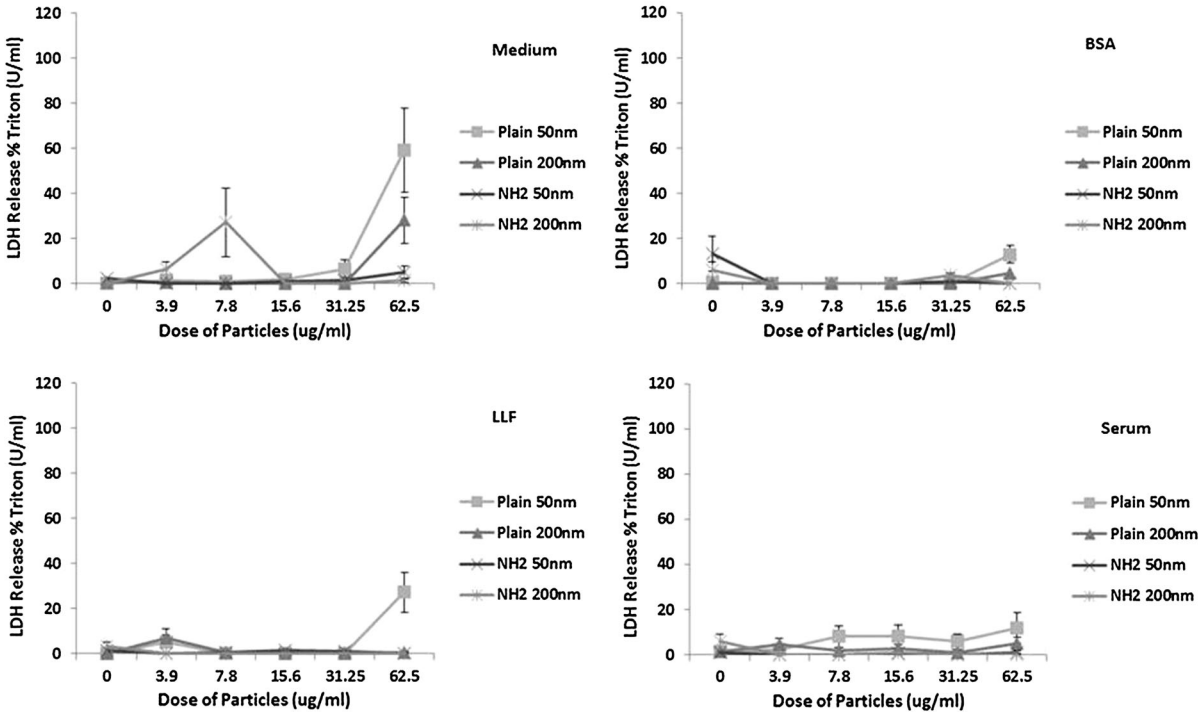

Fig. 3 LDH release from A549 cells treated with silica NPs dispersed in medium, BSA, LLF or serum for 24 h. Data represent the mean ± SEM of the number of units/ml of LDH released into the culture medium and expressed as a percentage of the total LDH remaining. Each experiment was carried out on three separate occasions

50 nm particles produced a significant ($p < 0.001$, $p < 0.05$ and $p < 0.01$, respectively) increase in the tail moment compared with untreated cells when dispersed in LLF. NH_2 200 nm particles had no effect. For plain 50 nm particles, the Fpg effect was not significantly different from the effect observed for plain 50 nm particles in the absence of Fpg. In general, dispersing the particles in LLF caused a significant ($p < 0.001$) reduction in the Fpg response compared with particles dispersed in HBSS.

When particles were dispersed in serum, there was a significant genotoxic effect on the A549 cells caused by plain 50 nm nanoparticles, both in the presence and absence of Fpg. The overall Fpg effect, however, was not significant.

Table 5 summarises the significant effects between different particles suspended in the different dispersants.

Plain 50 nm silica nanoparticles exhibited some toxicity at the higher dose of 62.5 μg/ml, although this effect was not statistically significant. We therefore repeated the comet assay with only this particle type suspended in the different dispersants to investigate whether the effects observed at the highest dose were evident at a lower dose of 31.25 μg/ml. The results are shown in Fig. 5.

Using a global ANOVA where we examined the effect of particle treatment and dispersant across all the data, we show that at a lower dose of plain 50 nm nanoparticles, there was a significant increase in the tail moment in particle-treated cells compared with untreated cells ($p < 0.001$). There was also a significant difference between Fpg-treated and non-Fpg-treated cells ($p < 0.001$). The largest differences were noted for particle treatments in the presence of Fpg. The tail moments of the cells treated with particles dispersed in BSA, LLF and serum were significantly less than those in the HBSS treatment ($p < 0.05$; $p < 0.001$; $p < 0.001$, respectively). Overall, there were significant differences between particles dispersed in HBSS and BSA ($p < 0.05$), LLF ($p < 0.001$) and serum ($p < 0.001$).

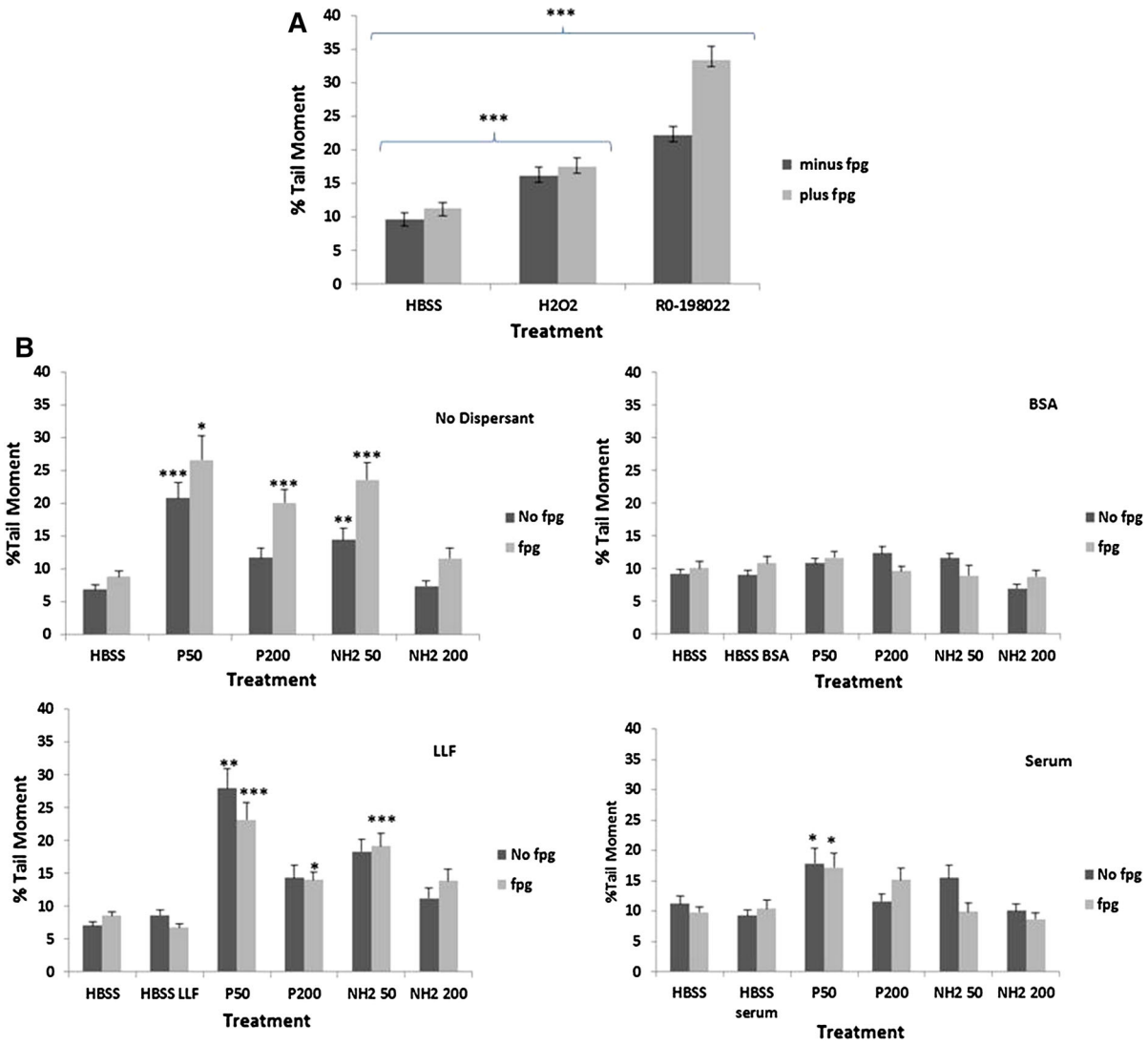

Fig. 4 DNA strand breaks in A549 cells after treatment with H_2O_2 and RO-198022 compound (*upper graph*) and with silica NPs (*lower graphs*). The *horizontal axis* treatments are represented as HBSS—no particles; P50—plain silica 50-nm-diameter particles; P200—plain silica 200-nm-diameter particles; NH_2 50—NH_2-modified silica 50-nm-diameter particles; and NH_2 200—NH_2-modified silica 200-nm-diameter particles. Individual graphs show the dispersant in which the particles were suspended. Data represent the mean ± SEM of the % tail moment (a total of fifty cells per treatment were measured in each experiment and each experiment was carried out on three separate occasions) $^*p < 0.05$; $^{**}p < 0.01$; $^{***}p < 0.001$ compared with the appropriate control

Micronucleus formation in A549 cells

Figure 6 shows the presence of micronuclei in A549 cells after cytochalasin B treatment. The images serve to illustrate the criteria used to count the micronuclei.

Micronuclei were counted using the protocol outlined in the materials and methods and the cytokinesis block proliferation index for each treatment shown in Table 6. Only one set of results was available for the BSA treatment.

Table 5 Summary of the significant effects between particles suspended in different dispersants

Treatment	Fpg	P50	P200	NH_2 50	NH_2 200
HBSS significant Fpg effect ($p < 0.001$)					
HBSS only	−	0.001	NSD	0.01	NSD
	+	0.05	0.001	0.001	NSD
P50	−	*	NSD	0.01	NSD
	+		NSD	NSD	0.05
P200	−		*	NSD	0.01
	+			NSD	0.001
NH_2 50	−			*	0.001
	+				0.001
NH_2 200	−				*
	+				
LLF significant Fpg effect ($p < 0.001$)					
LLF	−	0.001	NSD	0.001	NSD
	+	0.001	0.05	0.001	NSD
P50	−	*	0.001	NSD	0.01
	+		NSD	NSD	NSD
P200	−		*	0.01	NSD
	+			NSD	NSD
NH_2 50	−			*	0.01
	+				0.05
NH_2 200	−				*
	+				
Serum no significant Fpg effect					
Serum	−	0.05	NSD	NSD	NSD
	+	0.05	NSD	NSD	NSD
P50	−	*	NSD	NSD	0.05
	+		NSD	0.01	0.001
P200	−		*	NSD	NSD
	+			NSD	NSD
NH_2 50	−			*	NSD
	+				NSD
NH_2 200	−				*
	+				
BSA no significant Fpg effect					
BSA	−	NSD	NSD	NSD	NSD
	+	NSD	NSD	NSD	NSD
P50	−	*	NSD	NSD	0.05
	+		NSD	0.05	NSD
P200	−		*	NSD	0.001
	+			NSD	NSD
NH_2 50	−			*	0.001
	+				NSD
NH_2 200	−				*
	+				

Column and row labels refer to the particle treatment in each dispersant compared with each other particle type. NSD indicates no significant difference between the comparisons

* indicates that the comparison was not obtained

There were no significant differences in micronucleus formation regardless of the particle treatment, nor were there any differences when the particles were suspended in different dispersants.

Discussion

We investigated the effects of size, surface chemistry and dispersion medium on the ability of silica particles to produce genotoxic effects in A549 lung epithelial cells. The main focus of our study was to determine whether or not the dispersion medium could modulate the genotoxic effects of the particles. It has become apparent from the literature that studies using nanoparticles must be robust in terms of the characterisation techniques employed. Routinely, measurements such as DLS and zeta potential are used to characterise particles, as well as some form of microscopical techniques such as SEM or TEM. In addition, there has been considerable debate regarding the best way to disperse particles, and some studies have used artificial surfactants, sonication (Taurozzi et al. 2011) or dispersion of particles in organic solvents (Cook et al. 2010). In a comprehensive study by Corradi et al. (2012), the authors suggest that the protein corona acts as a protective layer. It is likely that the interactions between particle and protein are more complicated. The formation and the presence of a protein corona on different types of nanoparticle have been well described (Lesniak et al. 2010; Petri-Fink et al. 2008), and the modulatory effects including reduced toxicity and effects on phagocytosis of protein-coated nanomaterials are recognised. However, it has also been noted that these effects depend on a range of other factors such as cell type, concentration and type

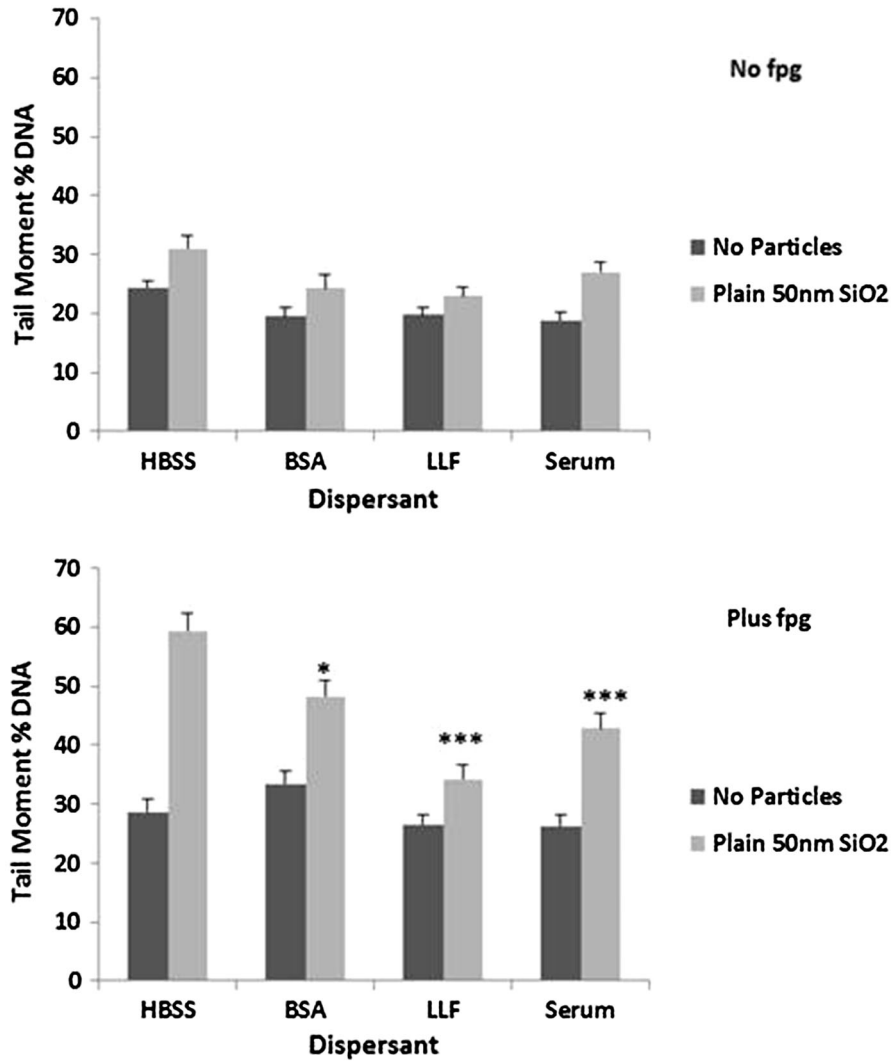

Fig. 5 DNA strand breaks in A549 cells after treatment with plain 50 nm (31.25 μg/ml) silica NPs dispersed in different media. Data represent the mean ± SEM of the % tail moment (a total of fifty cells per treatment were measured in each experiment and each experiment was carried out on three separate occasions) (*$p < 0.05$; **$p < 0.01$; ***$p < 0.001$ compared with HBSS)

of coating, incubation time and the chosen endpoint. For example, Clift et al. (2010) have described the effects of FCS on the bioactivity of 20 nm polystyrene beads using J774 cells and demonstrated that using the MTT assay, after 2-, 4- and 48-h treatment with and without FCS, the metabolic activity of the cells was not different. However, at 24 h the presence of FCS significantly reduced the metabolic activity of cells treated with 20 nm polystyrene beads at a dose of 50 μg/ml. In contrast, in both the presence and the absence of FCS, the LDH release was significantly increased. These observations indicate an important point in that the choice of endpoint should be carefully considered when choosing an assay for measuring cytotoxicity and that the dispersants in which the treatments are suspended can influence the outcome of such experiments.

Studies involving the use of superparamagnetic iron oxide nanoparticles (SPIONs) (Petri-Fink et al. 2008) have demonstrated the effect of an amine copolymer associated with the particles, and serum on cytotoxicity and uptake. This study highlights the comments mentioned previously regarding the complexity of interactions between particles, surface chemistry, particle coating and choice of cell type and endpoint. Here, the presence of serum was shown to inhibit the uptake of particles with an associated amine copolymer surface. In a more recent study,

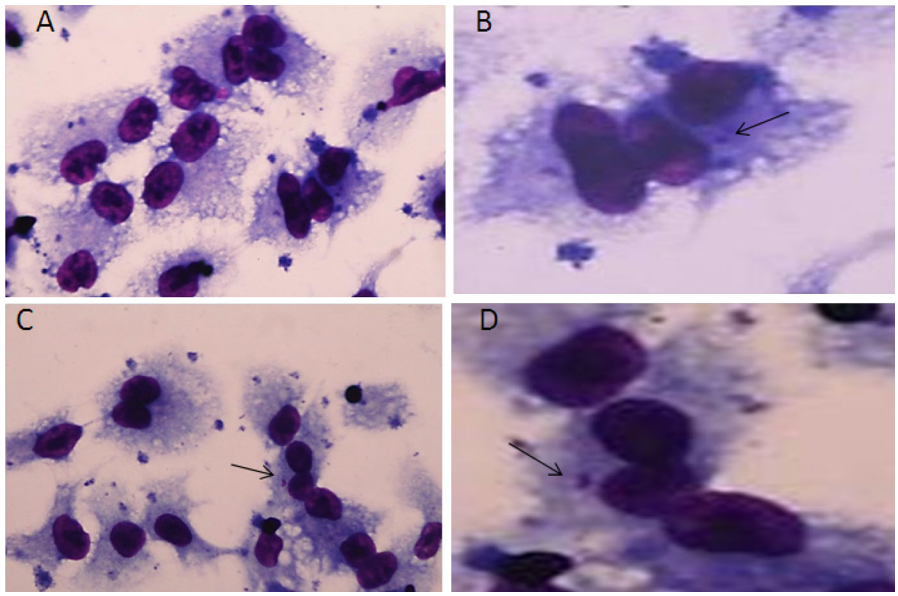

Fig. 6 A549 cells observed using oil immersion (×100) light microscopy. The *images* show several binucleated cells, indicating cell proliferation in the presence of cytochalasin B treatment. The *arrows* show binucleated cells with micronuclei. Several mononucleated cells are also observed, as well as a necrotic cell on the *top right corner* (**a**) and a cell undergoing apoptosis at the *bottom of the picture*. **b** and **d** are enlargements of the cells containing the micronuclei

Table 6 The cytokinesis block proliferation index (CBPI) calculated from micronucleus formation

Particle treatment	BSA	LLF	Serum
No particles	0.022	0.022 ± 0.003	0.027 ± 0.014
Plain silica 50 nm	0.047	0.02 ± 0.003	0.034 ± 0.013
Plain silica 200 nm	0.014	0.011 ± 0.004	0.027 ± 0.01
Silica NH_2 50 nm	0.046	0.021 ± 0.01	0.03 ± 0.014
Silica NH_2 200 nm	0.036	0.018 ± 0.01	0.022 ± 0.01

Two-hundred and fifty cells were counted per treatment for each particle type and is represented as the mean ± SEM

Panas et al. (2013) confirmed that cell viability was decreased in the absence of serum and consequently the particles were less toxic when dispersed in serum.

Our interest lies ultimately in the interaction of particles and proteins, in particular the route of entry of particles into the body and the consequences of this exposure to different organ systems of the body. For instance, uncoated silica particles entering the lung immediately become coated with proteins and other immunomodulatory molecules contained in LLF. This initial coating of the particle may be sufficient to produce local effects within the lungs themselves. The particles may interact with different cell types of the lung such as airway cells and cells in the alveolar region. That protein coatings of various kinds alter the reactivity of the particle surface is well established, and LLF certainly contains components of the complement system which act as opsonins to assist in particle clearance. However, particles which initially are coated with LLF in the lung may translocate via the bloodstream to organs distal to the lung and during this process encounter other proteins in blood such as albumin and serum proteins (Oberdorster et al. 2002). Here it should be considered that an additional coating of proteins from the blood may be formed on top of an existing coating obtained in the lung. The question arises whether or not this extra coating makes the particle more toxic or less toxic or stimulates cells in other ways. This question forms the basis of our future work.

In this study, one of our concerns was that the dispersion of particles should utilise medium which is biologically relevant to the in vivo scenario. We chose three different dispersants with different characteristics in terms of their protein and/or phospholipid profile to model the possible routes to which workers using nanomaterials may become exposed. Albumin and serum were selected as dispersants because of their relevance with respect to exposure to blood-borne particles and existing in vitro model protocols, and lung lining fluid due to its relevance to exposure of particles via the lung.

Our characterization data showed that the plain silica 50 and 200 nm particles were generally well dispersed in each medium type. In contrast, the 50 nm

aminated particles were overall more agglomerated than the 200 nm aminated particles when dispersed in medium, LLF or serum. The particle measurements obtained in water supported those provided by the manufacturers, and we suggest that the size differences we observed may be due to the corona formation on the particles by the components of the dispersants. As mentioned previously (Results section), in the examination of size distribution characteristics obtained by DLS, the smaller than expected particle diameter may be due to the presence of aggregates of dispersant material. The aminated particles may be expected to exhibit a relatively positive charge compared to the plain particles; however, no such difference was observed (when zeta potential measurements were made). This suggests that either the positive charge was masked by the medium components or that the aminated surface was not stable. The aminated particles also appeared to be more agglomerated than the plain particles, again suggesting a lack of significant charge. Interaction of the particles with different proteins and other biological molecules may affect the agglomeration of the particles as well as their sedimentation rate and hence the way they interact with the cells. The impact of coating may be relevant in vivo, where particles encounter serum proteins or in the lung where particles may interact with the components of LLF. The zeta potential measurements produced here suggest that all of the particles were agglomerated to some degree regardless of the medium used to disperse them, and the low zeta potentials associated with BSA and serum are possibly due to the proteins.

The toxicity of all of the silica particles suspended in the different dispersants at 4 and 24 h post exposure was not statistically significant, indicating the suitability of the dose range used. However, a slight but non-significant elevation of LDH release appeared to occur with the highest concentration (62.5 μg/ml) of plain 50 nm silica nanoparticles. Therefore, genotoxicity studies were repeated at a lower dose of 31.25 μg/ml in such cases in order to ensure that genotoxicity measured was not associated with cell death.

The modified comet assay was used to investigate the possible genotoxic effects of the particles in different dispersants on A549 cells. The enzyme Fpg was used to enhance assay sensitivity, since this enzyme detects DNA damage due to oxidative effects. This is a key enzyme in the base excision repair pathway, removing modified purines such as 8-oxoguanine and then cleaving the mutated DNA strand, so that on electrophoresis a larger comet tail is detected due to the extra DNA fragments and this increase is attributed to oxidative effects. Firstly, our data indicated that both 50 and 200 nm silica particles induced significant genotoxicity to the A549 cells and that there was a strong oxidative component to this effect. Plain 50 nm, plain 200 and 50 nm aminated silica particles produced a significant increase in the tail moment of cells exposed to these particles when dispersed in HBSS and LLF in the presence of Fpg. This effect was reduced or abolished when the particles were dispersed in serum or BSA. Both BSA and serum contain antioxidants which may account for this observation. Alternatively, binding of the albumin component of BSA and serum may have altered the surface reactivity of the particles, rendering them less reactive (Brown et al. 2012). There was also a significant increase in the tail moment in cells exposed to plain 50 nm and aminated 50 nm particles dispersed in medium in the absence of Fpg, suggesting that the smaller diameter particles were more reactive than the larger 200 nm particles. In LLF, only plain 50 nm particles dispersed in LLF in the absence of Fpg produced a significant increase in the tail moment compared with untreated cells. This suggests that for some particles, but not the aminated 50 nm particles, LLF can reduce the genotoxic potential. Our study also demonstrates that oxidative damage is also present at a lower dose using plain 50 nm silica particles (31.25 μg/ml), an effect which was reduced when the particles were dispersed in LLF, BSA and serum. These data therefore demonstrate that the dispersant used can influence the genotoxicity of particles in vitro. Furthermore, the data suggest the potential in vivo for body fluids to protect against genotoxicity induced by nanoparticles.

In previous studies using crystalline forms of silica (Fubini et al. 1990; Donaldson and Borm 1998; Shi et al. 1998; SaYotti et al. 1994; Daniel et al. 1995; Seiler et al. 2001), the role of oxidative stress in particle toxicity was demonstrated both in rat lung and in human lung epithelial cells. Similarly, Fanizza et al. (2007) demonstrated that α-quartz caused oxidative DNA damage in vitro, and this effect appeared to be related to the surface reactivity of the particle as well as the size and by an intracellular mechanism after the particles had been phagocytosed. The persistence of an

inflammatory response after particle-induced inflammation may result in the formation of reactive oxygen species which in turn may further promote DNA damage. Our data suggest that amorphous silica particles can also generate ROS effects in vitro. More specifically, the use of the Fpg enzyme when conducting the comet assay enables the detection of DNA damage mediated by oxidative processes. Our data demonstrated that DNA damage was enhanced when the comet assay was conducted in the presence of Fpg, indicating an involvement of ROS in silica NP-mediated genotoxicity. However, the production of ROS following NP exposure of A549 cells would need to be confirmed in a separate study. Many studies using the comet assay may detect genotoxicity in vitro but not in vivo as observed using TiO_2 (Bhattacharya et al. 2009; Warheit and Donner 2010).

As a comparison to the comet assay, we examined the effect of the silica particles on micronucleus formation in A549 cells. This assay appeared not to be as sensitive as the comet assay in detecting genotoxicity, as we found no significant changes in micronucleus formation with any of the particle treatments or when dispersed in different media. Moretti et al. (2002) suggested that a lack of sensitivity in the micronucleus assay compared with the comet assay may be due to differences in the actual type of damage to the cell. The authors hypothesized in their study that there may be differences in 'cytogenetic damage' as measured in the micronucleus assay compared with 'primary DNA damage' as measured using the comet assay. A similar scenario may be possible with the silica particles used here.

Conclusions

Our study suggests that plain 50 nm silica particles and aminated 50 nm silica particles are more reactive in producing DNA damage in A549 cells than the larger 200 nm particles, possibly through an oxidative mechanism. Amination appeared to have little influence over the genotoxicity of the silica nanomaterials. These effects can be modulated depending on the dispersion medium in which the particles are suspended, with albumin and serum quenching such effects. The study also stresses the significance of the dispersion medium on the agglomerated state of the particles that in turn may affect the particle surface–cell contact and the subsequent cellular responses to NPs.

Acknowledgments The authors are grateful to the Colt Foundation for continued support.

References

Balbus JM, Maynard AD, Colvin VL, Castranova V, Daston GP, Denison RA et al (2007) Meeting report: hazard assessment for NPs—report from an interdisciplinary workshop. Environ Health Perspect 115(11):1654–1659

Baughman RP, Mangels DJ, Strohofer S, Corser BC (1987) Enhancement of macrophage and monocyte cytotoxicity by the surface active material of lung lining fluid. J Lab Clin Med 109(6):692–697

Bhattacharya K, Davoren M, Boertz J, Schins RP, Hoffmann E, Dopp E (2009) Titanium dioxide nanoparticles induce oxidative stress and DNA-adduct formation but not DNA-breakage in human lung cells. Part Fibre Toxicol 6:17

Brown DM, Wilson MR, MacNee W, Stone V, Donaldson K (2001) Size-dependent proinflammatory effects of ultrafine polystyrene particles: a role for surface area and oxidative stress in the enhanced activity of ultrafines. Toxicol Appl Pharmacol 175:191–199

Brown DM, Dickson C, Duncan P, Al-Attili F, Stone V (2012) Interaction between NPs and cytokine proteins: impact on protein and particle functionality. Nanotechnology 21: 215104

Casals E, Puntes VF (2012) Inorganic nanoparticle biomolecular corona: formation, evolution and biological impact. Nanomedicine 7(12):1917–1930

Clift MJD, Bhattacharjee S, Brown DM, Stone V (2010) The effects of serum on the toxicity of manufactured nanoparticles. Toxicol Lett 198:358–365

Cook SM, Aker WG, Rasulev BF, Hwang HM, Leszczynski J, Jenkins JJ et al (2010) Choosing safe dispersing media for C60 fullerenes by using cytotoxicity tests on the bacterium Escherichia coli. J Hazard Mater 176(1–3):367–373

Corradi S, Gonzalez L, Thomassen LCJ, Bilanicova D, Birkedal RK, Pojana G et al (2012) Influence of serum on in situ proliferation and genotoxicity in A549 human lung cells exposed to nanomaterials. Mutat Res 745:21–27

Daniel LN, Mao Y, Safiotti U (1995) Direct interaction between crystalline silica and DNA: a proposed model for silica carcinogenesis. Scand J Work Environ Health 21(2):22–26

Donaldson K, Borm PJA (1998) The quartz hazard: a variable entity. Ann Occup Hyg 42:287–294

Ehrenberg MS, Friedman AE, Finkelstein JN, Oberdörster G, McGrath JL (2009) The influence of protein adsorption on nanoparticle association with cultured endothelial cells. Biomaterials 30(4):603–610

Fanizza C, Ursini CL, Paba E, Ciervo A, Di Francesco A, Maiello R et al (2007) Cytotoxicity and DNA-damage in human lung epithelial cells exposed to respirable alpha-quartz. Toxicol Vitro 21(4):586–594

Fröhlich E (2012) The role of surface charge in cellular uptake and cytotoxicity of medical nanoparticles. Int J Nanomed 7:5577–5591

Fubini B, Giamello E, Volante M, Bolis V (1990) Chemical functionalities at the silica surface determining its reactivity when inhaled. Formation and reactivity of surface radicals. Toxicol Ind Health 6:571–598

Greenwood R, Kendall K (1999) Selection of suitable dispersants for aqueous suspensions of zirconia and titania powders using acoustophoresis. J Eur Ceram Soc 19(4):479–488

Jani PU, Halbert GW, Langridge J, Florence AT (1990) Nanoparticle uptake by the rat gastrointestinal mucosa: quantitation and particle size dependency. J Pharm Pharmacol 42:821

Lesniak A, Campbell A, Monopoli MP, Lynch I, Salvati A, Dawson KA (2010) Serum heat inactivation affects protein corona composition and nanoparticles uptake. Biomaterials 31(36):9511–9518

Lipka J, Semmler-Behnke M, Sperling RA, Wenk A, Takenaka S, Schleh C, Kissel T, Parak WJ, Kreyling WG (2010) Biodistribution of PEG-modified gold nanoparticles following intratracheal instillation and intravenous injection. Biomaterials 31:6574

Lundqvist M, Stigler J, Cedervall T, Berggård T, Flanagan MB, Lynch I et al (2011) The evolution of the protein corona around nanoparticles: a test study. ACS Nano 5(9):7503–7509

Moretti M, Maracarelli M, Villarini M, Fatigoni C (2002) In vitro testing of the herbicide terbutryn: cytogenetic and primary DNA damage. Toxicol Vitro 16:81–88

Nel AE, Madler L, Velegol D, Xia T, Hoek EM, Somasundaran P et al (2009) Understanding biophysicochemical interactions at the nano-bio interface. Nat Mater 8:543–557

Oberdorster G, Sharp Z, Atudorei V, Elder A, Gelein R, Lunts A, Kreyling W, Cox C (2002) Extrapulmonary translocation of ultrafine carbon particles following whole-body inhalation exposure of rats. J Toxicol Environ Health 65:1531–1543

Oberdorster G, Maynard A, Donaldson K, Castranova V, Fitzpatrick J, Ausman K et al (2005) Principles for characterizing the potential human health effects from exposure to nanomaterials: elements of a screening strategy. Part Fibre Toxicol 2:8–43

Panas A, Marquardt C, Nalcaci O, Bockhorn H, Baumann W, Paur HR et al (2013) Screening of different metal oxide nanoparticles reveals selective toxicity and inflammatory potential of silica nanoparticles in lung epithelial cells and macrophages. Nanotoxicology 7(3):259–273

Petri-Fink A, Steitz B, Finka A, Salaklang J, Hofmann H (2008) Effect of cell media on polymer coated superparamagnetic iron oxide nanoparticles (SPIONs): colloidal stability, cytotoxicity and cellular uptake studies. Eur J Pharm Biopharm 68:129–137

Rothen-Rutishauser B, Brown DM, Piallier-Boyles M, Kinloch IA, Windle AH, Gehr P et al (2010) Relating the physiochemical characteristics and dispersion of multiwalled carbon nanotubes to their oxidative reactivity in vitro and inflammation in vitro. Nanotoxicology 4(3):331–342

SaYotti U, Daniel LN, Mao Y, Shi X, Williams AO, Kaighn ME (1994) Mechanisms of carcinogenesis by crystalline silica in relation to oxygen radicals. Environ Health Perspect 102(10):159–163

Schleh C, Semmler-Behnke M, Lipka J, Wenk A, Hirn S, Schäffler M, Schmid G, Simon U, Kreyling WG (2012) Size and surface charge of gold nanoparticles determine absorption across intestinal barriers and accumulation in secondary target organs after oral administration. Nanotoxicology 6:36–46

Seeberg E, Eide L, Bjørås M (1995) The base excision repair pathway. Trends Biochem Sci 20(10):391–397

Seiler F, Rehn B, Rehn S, Bruch J (2001) Quartz exposure of the rat lung leads to a linear dose response in inflammation but not in oxidative DNA damage and mutagenicity. Am J Respir Cell Mol Biol 24:492–498

Shi X, Castranova V, Halliwell V, Vallyathan V (1998) Reactive oxygen species and silica-induced carcinogenesis. J Toxicol Environ Health B1:181–197

Stone V, Shaw J, Brown DM, Macnee W, Faux SP, Donaldson K (1998) The role of oxidative stress in the prolonged inhibitory effect of ultrafine carbon black on epithelial cell function. Toxicol Vitro 12(6):649–659

Taurozzi JS, Hackley VA, Wiesner MR (2011) Ultrasonic dispersion of nanoparticles for environmental, health and safety assessment–issues and recommendations. Nanotoxicology 5(4):711–729

Warheit DB, Donner EM (2010) Rationale of genotoxicity testing of nanomaterials: regulatory requirements and appropriateness of available OECD test guidelines. Nanotoxicology 4:409–413

Wilsher ML, Hughes DA, Haslam PL (1988) Immunoregulatory properties of pulmonary surfactant: effect of lung lining fluid on proliferation of human blood lymphocytes. Thorax 43:354–359